Article

Predicting Soil Erosion Rate at Transboundary Sub-Watersheds in Ali Gharbi, Southern Iraq using RUSLE based GIS-Model

Ammar Ak. Ali[1, 2], Alaa M. Al-Abbadi[1*], Fadhil K. Jabbar[3], Hassan Alzahrani[4*] , Samie Hamad[5]

[1] Department of Geology, College of Science, University of Basrah, Basrah, Iraq; alaa.atiaa@uobasrah.edu.iq (A.M.)
[2] General Commission of Groundwater, Ministry of Water Resoruces, Iraq; ammargeo76@gmail.com (A.A.)
[3] General Commission of Groundwater, Ministry of Water Resoruces, Iraq/ University of Misan, College of Engineering; drfkjabbar@uomisan.edu.iq (F.K.)
[4] Department of Geology and Geophysics, College of Science, King Saud University, 11451 Riyadh, Saudi Arabia; hsan@ksu.edu.sa (H.A.)
[5] Geological Engineering Department, Missouri University of Science and Technology, McNutt Hall, 1400 N. Bishop Ave, Rolla, MO 65401, USA; sraf35@umsystem.edu (S.H.)
* Correspondence: alaa.atiaa@uobasrah.edu.iq, hsan@ksu.edu.sa

Abstract: The empirical soil loss model, RUSLE, was used with conjunction of remotely sensed data and geographic information system technology to delineate the soil erosion and watershed priorities in terms of conservation practices at seven boundary sub-watersheds (labeled as SW-00, SW-01, …, SW-06) between Iraq and Iran at Ali Al-Gharbi area, southern Iraq. The six factors of the RUSLE model, ie. the rainfall erosivity, the soil erodibility, the slope steepness length, the crop management, and management practice, were calculated or estimated using information from different data sources such as remotely sensed data and previous studies. Finding showed that the annual soil erosion loss ranges from 0 - 1890 (tons h-1 y-1) with an average of 0.66 (tons h-1 y-1). Values of soil erosion were classified into five classes: very low, low, moderate, high, and very high. The potential soil loss in the high and very high classes ranges from 14.84 to 1890 (tons h-1 y-1), and these classes occupy only 27 km2 of the study area, indicating that the soil loss is very low in the area being examined. In terms of the spatial distribution of soil loss, the northern and northeastern parts (mountains and hills) of the sub-watersheds where the slope is steeper are more likely to erode than the plain area in the southern and southeastern portions, indicating that slope, in addition to rainfall erosivity, has a dominant effect on the soil erosion rate. The study of soil erosion in the watersheds under consideration reveals that only the northern portions of the SW-00, SW-02, and SW-04 watersheds require high priority conservation plans; however, these portions are primarily located in mountain regions, making conservation plans implementation in these areas impractical. Due to low soil loss, other sub-watersheds, particularly SW-01, SW-03, SW-05, and SW-06, are given low priority.

Keywords: Soil erosion; GIS; RUSLE model; Iraq

1. Introduction

Watersheds are globally facing significant environmental challenges like extreme climate changes, droughts, floods, and intensive agriculture practices that cause soil erosion. The impact of all these challenges deteriorates the soil and water quality of the watershed, on which the sustainability and productivity of the watershed depend. Environmental processes in a watershed are all interdependent where the change in one can influence the other. The process of soil erosion is the detachment and transport of soil particles due to erosion forces. The forces of erosion may be caused by wind, ice, or water, such as raindrops or surface runoff [1-4]. In addition to reducing soil fertility and soil degradation, soil erosion has a negative influence on the sustainability and productivity of agricultural areas

 doi:10.20944/preprints202211.0298.v1

[5,6]. A decrease in soil fertility is also a consequence of soil erosion, which has caused water quality problems and a threat to sustainable agriculture [7].

Prioritizing watersheds is a procedure for identifying environmentally stressed sub-watersheds to take action for soil conservation. The process of prioritizing a watershed involves ranking different micro-watersheds in order of their treatment with suitable soil conservation measures [8]. Therefore, prioritizing sub watersheds will help in their efficient adoption and allocation resources on the priority basis [9]. The degradation of land is not the only consequence of erosion; it also directly impacts watershed health by affecting quality and quantity of water. By carrying the loose soil with it, water causes erosion, reducing the storage capacity and life of reservoirs and dams [10] and directly effects watershed health.

To quantify soil erosion many empirical models suitable for ungagged basins were developed in the past. For instance, soil erosion models such as the Soil and Water Assessment Tool (SWAT) [11], EROSION 3D [12], universal soil loss equation (USLE)[13] or its revised version (RUSLE)[14] have been broadly applied around the world.

In recent years, the integration of RUSLE model with geospatial modeling, geographic information systems, and satellite imagery data has led to its widespread use in assessing soil erosion on a regional scale in a cost-effective and accurate manner [15-19].

On the basis of the results of its simplified structure and ease of incorporating parameters, The RUSLE model was applied by many researchers to estimate the most vulnerable zones that can be potential sources of sediments and estimate volumes of the sediments load for any basin [20-24]. For instance, this technique has been conducted to predict soil erosion by combining and extracting some parameters of the RUSLE model with Google Earth Engine[25]. Alternatively, other studies have been conducted to evaluate soil erosion loss in different regions by utilizing remote sensing (RS) and Geographical Information System (GIS) techniques besides using the empirical soil erosion model [26,27]. Soil erosion models will provide useful information including soil erosion evaluation and monitoring for any wide area [28-30]. Therefore, the quality of the outputs for the models is variable depending on the difference in the computational approaches and the number of required inputs.

Given the economic significance of the Ali Al-Gharbi, northern Mayan Governorate, southern Iraq as a promising agricultural region and the likelihood of land degradation due to natural (soil erosion) and anthropogenic factors, this study area necessitates comprehensive studies to establish management practices and determine the priorities of the watersheds. Therefore, in this study, seven transboundary (between Iraq and Iran) sub-watersheds (transboundary sub-watersheds) were assessed to priority watersheds in terms of soil erosion using RULSE model. The results of RULSE model were used a guide to initiate conservation plans in the study area to protect land and agricultural areas. The spatiotemporal variation of soil erosion for the four years 2017, 2018, 2019, and 2020 were evaluated to determine how the temporal variation of soil erosion as a result of rainfall and LULC variation over the basin may influence watershed priority.

2. Materials and Methods

2.1. The study area

The seven sub-watersheds are located between Iraq and Iran and cover an area of approximately 3770 km², (Figure 1). The main watershed spans a large portion of western Iran (Ilam province) and northeastern Maysan Governorate in Iraq. The study area contains several relatively large valleys as well as numerous smaller ones. The majority of these valleys, which flow eastward towards Iraq, are found in western Iran. The catchment area in Iraq is mostly flat land with elevations ranging from 25 meters at the southeast end to 400 meters at the international border. The Iranian portion of the basin, on the other hand, is comprised of high lands with elevations exceeding 2500 meters. The majority of it is made up of hills and mountains, and the highest points of the mountains mark the division of the catchment area [31].

Preprints (www.preprints.org) | NOT PEER-REVIEWED | Posted: 16 November 2022 doi:10.20944/preprints202211.0298.v1

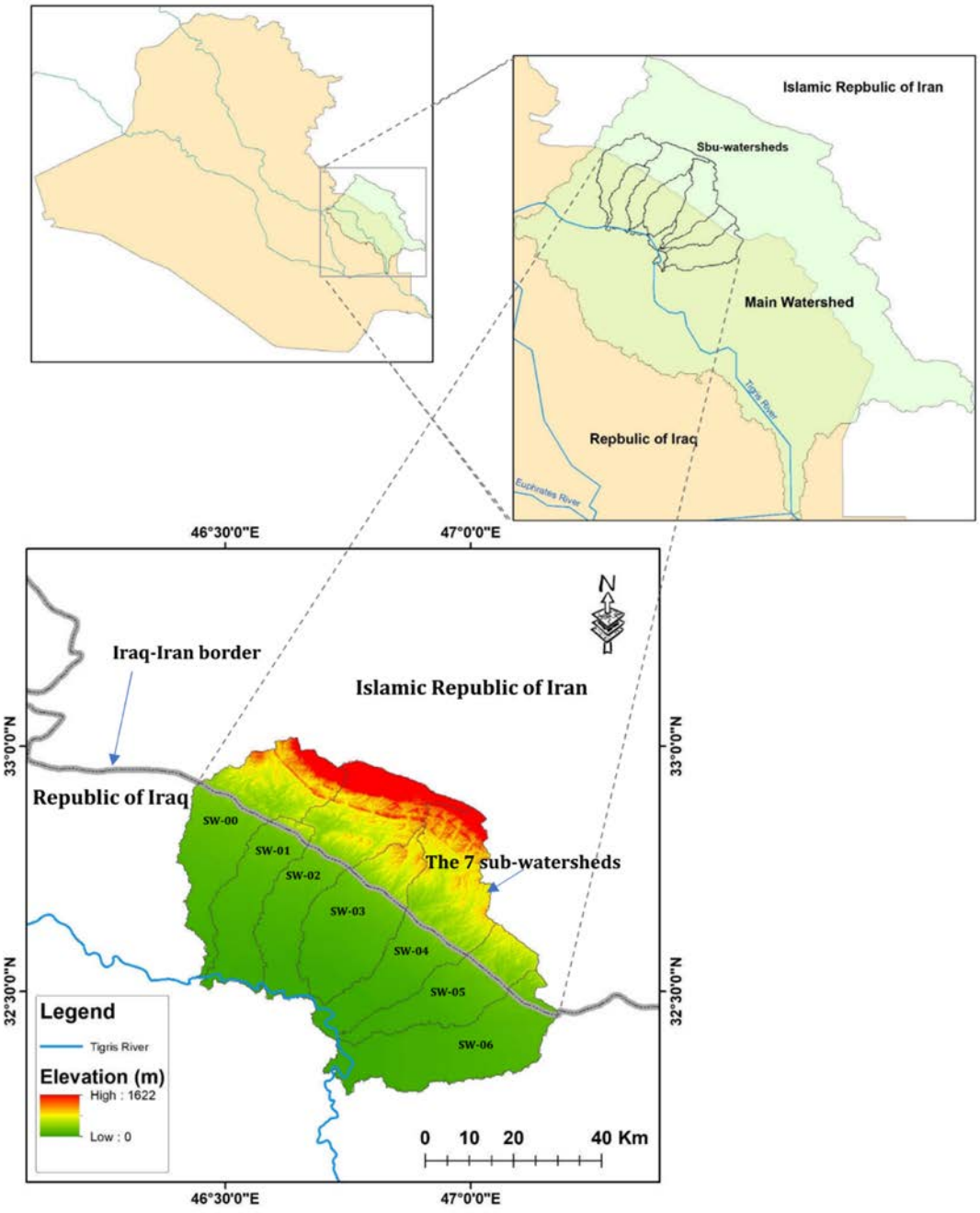

Figure 1. Location of the study area.

Subtropical desert climate (Köppen-Geiger type BWh) predominates in the watershed's Iraqi portion, and hot semi-arid climate (Köppen-Geiger type BSh) predominates in the watershed's Iranian portion. The average yearly temperature for Ali Al-Gharbi is 30.79 °C, which is 4.02 percent higher than the national average for Iraq. There are 32.41 rainy days on average each year, with annual precipitation totaling 16.85 mm. The sub-northern most watershed's region, Dehloran in Iran, experiences daytime highs of 19°C and nighttime lows of 11°C. 20.48 mm of rain falls on average each year, and the humidity level is very close to 41%. According to the digital soil map of the world [32], the three main soil types in the study area are clay loam, loam, and sand, (Figure 2). For clay loam, loam, and sand, respectively, the three textures occupy 1257 km² (33%), 2090 km² (55%), and 423 km² (11%) of total land area. The soil is highly permeable, resulting in high infiltration rates and low runoff, according to the distribution of loam and sand textures that

Preprints (www.preprints.org) | NOT PEER-REVIEWED | Posted: 16 November 2022 doi:10.20944/preprints202211.0298.v1

belong to the B and A hydrological groups. The study area's northern and eastern portions are covered in loam and sandy soils, while the middle and majority of the southern part are covered in clayey loam, suggesting that these regions are likely to experience runoff and flooding and thus it more vulnerable to soil loss.

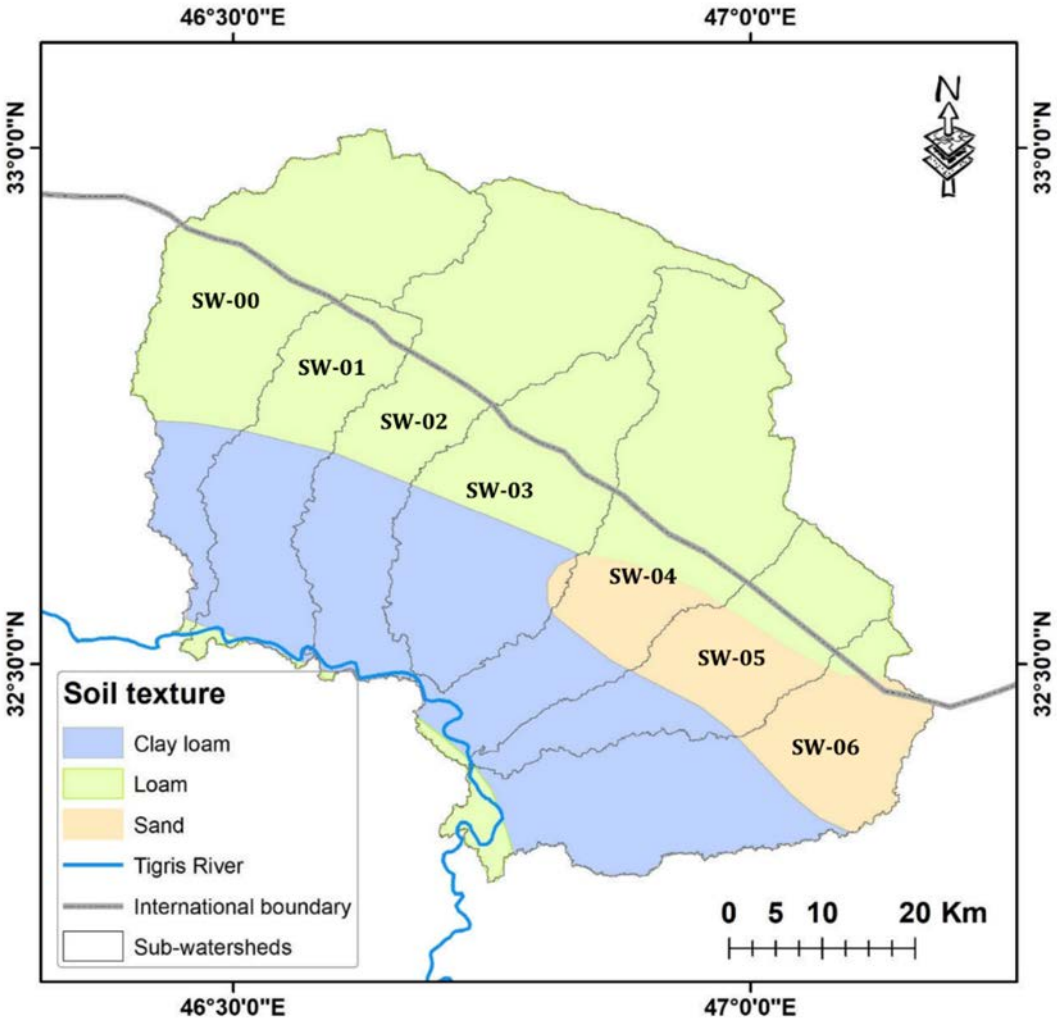

Figure 2. Soil texture map.

The Mesopotamian Foredeep basin and a small portion of the Zagros Fold belt occupy the Iraqi portion of the research area, whereas the Zagros Fold Belt encompasses the Iranian territory (Figure 2). The Mesopotamian Foredeep basin is an elongated epicontinental basin that formed over an earlier continental or migration basin [33]. It has buried structures such as folds, faults, and diapiric structures. The Zagros fold belt is a zone of deformed crustal rocks formed by the collision of the Arabian margin and the Eurasian plate following the closure of the Neo- Tethys Ocean during the Tertiary [34,35].

2.2. Techniques and data used

A wide selection of data was acquired from different sources as listed in Table 1. These include a digital elevation model (DEM) at 30 m resolution, crop management factor (C), Erosivity Database, land use, soil, as well as meteorological data. The geoprocessing tools within ArcGIS 10.8.1 software were applied to resample and calculate slope using elevation data with resolution (30 m × 30 m) of all original data.

Table 1. List of data used in the current study.

 doi:10.20944/preprints202211.0298.v1

Type of Data	Spatial Resolution	Source
Digital Elevation Model (DEM)	30 m × 30 m	USGS. http://earthexplorer.usgs.gov/
Crop Management Factor (C)	10m x 10m	http://www.omafra.gov.on.ca/english/engineer/facts/12-051.htm
Erosivity Database	1 km x 1Km	European Soil Data Center (ESDAC) (https://esdac.jrc.ec.europa.eu/content/global-rainfall-erosivity#tabs-0- des criptio n=1)
Land Use/Land Cover (LULC)	10m x 10m	Sentinel-2 10m Land Use/Land Cover Time Series https://www.arcgis.com/apps/mapviewer/index.html?layers=d3da5dd386d140cf93fc9ecbf8da5e31
Soil	Vector unit	Sanchez et al., 2009; https://www.fao.org/soils-portal/data-hub/soil-maps-and-databases/en/
Meteorological Data	Weather station	NOAA, http://gis.ncdc.noaa.gov/

3. Results

Water erosion occurs when soil particles are detachment, transported, and deposited. Raindrops impacting the surface and water flowing over it are the major forces affecting water erosion. The factors affecting erosion can be calculated by using Equation (1) [36]:

$$E = f(C, S, T, SS, M) \quad (1)$$

where E means erosion, C is climate, S is soil properties, T is topography, SS is soil surface conditions, and M is human activities.

RUSL is a function relationship expressed by Equation (2) [13]:

$$A = R \cdot K \cdot LS \cdot C \cdot P \quad (2)$$

where A is the average annual soil loss (tons ha^{-1} year^{-1}), R is the rainfall erosivity (MJ mm ha^{-1} h^{-1} year^{-1}), K is the soil erodibility factor (tons ha^{-1}, h^{-1}, MJ mm^{-1}), LS is the slope length-steepness factor (dimensionless), C is the cropping management factor (dimensionless), and P is the practice support factor (dimensionless).

RUSLE equation aims to guide conservation planning by providing methodical guidelines. With the aid of the equation, the planner is capable of predicting the average rate of soil erosion on any given site for every possible combination of cropping systems, management strategies, and erosion control measures.

3.1. Rainfall erosivity (R)

Basically, R is a measure of how much erosion, rain could cause. R is the most crucial component for calculating erosion with RUSLE, according to a number of studies [13,37-38] and has a strong correlation with soil loss at many rain-station locations throughout the globe. It defined as product of the maximum intensity of rainfall over a 30 minutes and the kinetic energy of rainfall storm event [13]:

$$R = \frac{1}{n}\sum_{j=1}^{n}\sum_{k=1}^{m_j}(EI_{30})_k \quad (3)$$

Preprints (www.preprints.org) | NOT PEER-REVIEWED | Posted: 16 November 2022 doi:10.20944/preprints202211.0298.v1

where n is the number of years included in the analysis, m_j is the number of erosive events during year j, and EI_{30} (MJ mm ha-1 h-1) is the R for event k.

For a particular event, erosivity is calculated as follows:

$$EI_{30} = \left(\sum_{r=1}^{m} e_r \cdot v_r\right) \cdot I_{30} \quad (4)$$

where e_r is the kinetic energy per unit of rainfall (MJ ha^{-1} mm^{-1}); v_r is the rainfall depth (mm) for the hydrograph's time interval r; r is subdivide into m subintervals; I_{30} is the maximum rainfall intensity for a 30-minute timeframe.

In ungagged watersheds such as the considered study area, Equations (3 and 4) require information rarely found. Therefore, in this study, the **Glo**bal **R**ainfall **E**rosivity **Da**tabase (GloREDa) [39] was used to map the R in the unit of (MJ mm ha^{-1} h^{-1} yr^{-1}) over the study area. Approximately 3625 stations from 63 countries are included in the GloREDa to estimate the erosivity values as R-factors.

The global erosivity map of GeoTIFF format type at ~ 1 km spatial resolution is available for free download in the European Soil Data Center (ESDAC) (https://esdac.jrc.ec.europa.eu/content/global-rainfall-erosivity#tabs-0- des criptio n=1).

To obtain the spatial distribution of R in the study area, the global raster map of R was first downloaded from the previous website after completing a request form, and then extracted with a mask of the study area, reprojected, and then resample to 30m resolution in ArcMap 10.8.1 software.

3.2. Soil erodibility (K)

Basically, K is the degree to which a soil is erodible by raindrops and runoff. It is the product of susceptibility of soil particles to erosion per unit of rain erosivity factor (R) for a specified soil on a unit plot, which is defined as a 22.13 m length of uniform 9% slope continuously in clean-tiled fallow [40]. Although soil texture is the main factor affecting K, organic matter, structure, and permeability are also important. The typical values of K are between 0.02 to 0.69 (tons ha^{-1}, h^{-1}, MJ mm^{-1}). The K factor for the study area was estimated using the FAO global soil map [32] and its database in addition to the table provided by Roose (1996)[41], (Table 2).

3.3. Topographic factor

Topographic factors LS consists of slope length (L) and slope steepness (S). L, which is the ratio of soil loss from the field slope length to that from a 22.1m length of the same soil type and gradient, is used to represent the influence of slope length on erosion [42]. It denotes the distance from the source of overland flow to the point of concentration or deposition. Due to the gradual accumulation of runoff downslope with increasing L, erosion increases. S, on the other hand, represents erosion due to slope steepness. It is defined as the ratio of soil loss caused by the field gradient to that caused by a 9% slope under otherwise similar circumstances [43]. It is more rapid for soil loss to increase with slope steepness than with slope length.

The easiest way to calculate LS is through using DEM and hydrologic analysis. The following equations were used to calculate L, S, and LS [42]:

$$L = [(FA \times raster\ cell\ size)/22.13]^m \quad (5)$$

$$S = [(sin\beta \times 0.01745)/0.09]^n \quad (6)$$

$$LS = (L \times S)/100 \quad (7)$$

 doi:10.20944/preprints202211.0298.v1

where *FA* is flow accumulation layers produced by hydrologic analysis, cell size represents the DEM cell size, *m* ranges from 0.2-0.6, β is slope angle in %, and *n* ranges from 1.0-1.3.

Table 2. Estimating K based on soil texture and organic material content [41].

Textural class	Soil composition			Mean *K* (based on % organic material)		
	Sand	Silt	Clay	Unknown	< 2%	≥ 2%
Clay	0-45	0-40	40-100	0.22	0.24	0.21
Sandy Clay	45-65	0-20	35-55	0.20	0.20	0.200
Silty Clay	0-20	40-60	40-60	0.26	0.27	0.26
Sand	68-100	0-14	0-10	0.02	0.03	0.01
Sandy Loam	50-70	0-50	0-20	0.13	0.14	0.12
Clay Loam	20-45	15-52	27-40	0.30	0.33	0.28
Loam	23-52	28-50	7-27	0.30	0.34	0.26
Loamy San	70-86	0-30	0-15	0.04	0.05	0.04
Sandy Clay Loam	45-80	0-28	20-35	0.20	0.20	0.20
Silty Clay Loam	0-20	40-73	27-40	0.32	0.35	0.30
Silt	0-20	88-100	0-12	0.38	0.41	0.37
Silty Loam	20-50	74-88	0-27	0.38	0.41	0.37

Note: the table in the FAO soil database accounts for % organic matter (OM), not just organic carbon (OC). The value of OC should be multiplied by 1.72 to get OM.

3.4. Crop management factor (C)

C factor refers to the ratio of soil loss from cultivated land compared to fallow, clean-tilled land in specified conditions [40,44]. The *C* factor will indicate how the conservation plan will contribute to soil loss and how that soil loss might be distributed over time. This factor describes the impact of vegetation and erosion control practices on soil loss. Its value ranges from 0 in water bodies to slightly greater than 1 in bare land [45]. In the present study, the *C* factor values have been assigned from already available studies such as USLE fact sheet (http://www. omafra.gov.on.ca/english/engineer/facts/12-051.htm), U.N, Food and Agriculture Organization (http://www.fao. org/docrep /T1765E/ t1765e0c.htm), and RUSLE handbook[46]. Table 3 shows the typical values *C* factor for the LULC derived from ESRI 10m sentinel data.

Table 3. LULC derived from ESRI 10m sentinel data and associated *C* values.

LULC class number	Class name	C value
1	Water	0
2	Trees	0.025
4	Flooded Vegetation	1
5	Crops	0.05
7	Build Area	1
8	Bare Ground	1
9	Snow/ice	0
10	Clouds	0
11	Rangeland	0.4

3.5. Practice support factor (P)

The ratio of soil loss at a site caused by surface conditions to soil loss from uphill and downhill cultivation is known as the P factor [40]. The lower the *P* value, the more effective the conservation measure at reducing soil erosion is thought to be. The *P* factor

 doi:10.20944/preprints202211.0298.v1

value is set to 1 for the entire study region because no data on management practices for the relevant area is available.

4. Discussion

The calculated rainfall erosivity (*R)* values range 184 – 423 with an average of 626 (MJ mm ha^{-1} h^{-1} yr^{-1}). Spatially, rainfall erosivity *(R)* increases from southwest toward northeast as shown in Figure 3. The low and moderate *R* values are distributed in the Iraqi portions of watersheds, whereas the high and very high *R* values are located in the Iranian mountain parts of watersheds. Specifically, the R factor strongly correlates with the decreasing trend of elevation and rainfall in the northern and eastern parts of the study area [47] . For each soil mapping unit, SNUM is a sequential number linking soil information at the first level to the expansion file, the sequence of a sequential code ranges from 1 to 6,999, some numbers have not been used.

As illustrated in Table 4, the estimated soil erodibility (K factor) values for the study area range 0.04 to 0.33 with an average of 0.22 (tons ha^{-1} h^{-1} MJ mm^{-1}). The spatial distribution of *K* in the study area is depicted in Figure 3, from which it can be concluded that low values of *K* are distributed in the study area's center, while moderate and high values are concentrated in the northern and southern parts of the considered watersheds. Consequently, the middle parts of the study area are less likely to experience erosion than the rest of the study area. Therefore, K factor values reflect a compound relationship between soil physical properties and their impact on increasing soil erosion [48-50]. The type of DEM used to generate LS factor for the purpose of this study was SRTM with a spatial resolution of 30m. Based on the generated *LS* factor rater layer for the study area (Figure 4), it can be said that the northern regions of the study area are more vulnerable to soil erosion. However, soil erosion increases due to the gradual accumulation of runoff downslope with increasing slope length [51,52]. According to the calculated *LS* values, the study area is less prone to soil erosion except where the slopes are high in the mountains and hills. The *C* values for four node years (2017, 2018, 2019, and 2020) were mapped using Table 3 to show how the LULC variation affects the distribution of *C* over the study area (Figure 5). The *C* value range of (0.83 -1) decreases as the years proceed, and lowest spatial extension of this range was found in the years 2019 and 2020 due to the dominance of the rangeland (shrub) class over bare ground and crop LULC classes. In many cases, the potential erosion of rangeland is changed with time due to either particular management practices or natural cyclic impacts like growth during winter and spring [53,54].

To map soil erosion for the four node years, the raster calculator of ArcGIS 10.8.1 was used. The calculated soil erosion in (tons h^{-1} y^{-1}) for the four node years were classified into five classes using natural break classification scheme[55]: very low, low, moderate, high, and very high. The natural breaks scheme is a data clustering method that determines the best classification of values by minimizing each class's average deviation from the class mean while maximizing each class's deviation from the means of the other groups. Based on the RUSLE model, the maximum yearly soil loss was estimated to be 1890 (tons h^{-1} y^{-1}), for all node years, as shown in the results (Figure 6). In spite of the minor changes in *C* and the dominance of rangeland in the years 2019 and 2020 over bare ground and crop classes, soil loss remains the same and within the range 0 - 1890 (tons h^{-1} y^{-1}). There was potential loss in two classes ranges from 14.84 to 1890 (tons h^{-1} y^{-1}), and these classes occupy only 27 km^2 of the study area which indicates that the soil loss is very low in the area being examined. There is the highest risk for soil loss in the northern portion of the study area, because of the steep slopes. The high slope areas of the study area erode significantly more rapidly than the level areas in the southern part[56,57], and this may explain why soil erosion is relatively high there.

The study of soil erosion in the considered watersheds reveals that only the northern portions of the SW-00, SW-02, and SW-04 watersheds require high priority conservation

Preprints (www.preprints.org) | NOT PEER-REVIEWED | Posted: 16 November 2022 doi:10.20944/preprints202211.0298.v1

plans; however, these portions are primarily located in mountain regions, making implementation of conservation plans in these areas impractical. Other sub-watersheds, particularly SW-01, SW-03, SW-05, and SW-06, are given low priority due to low soil loss.

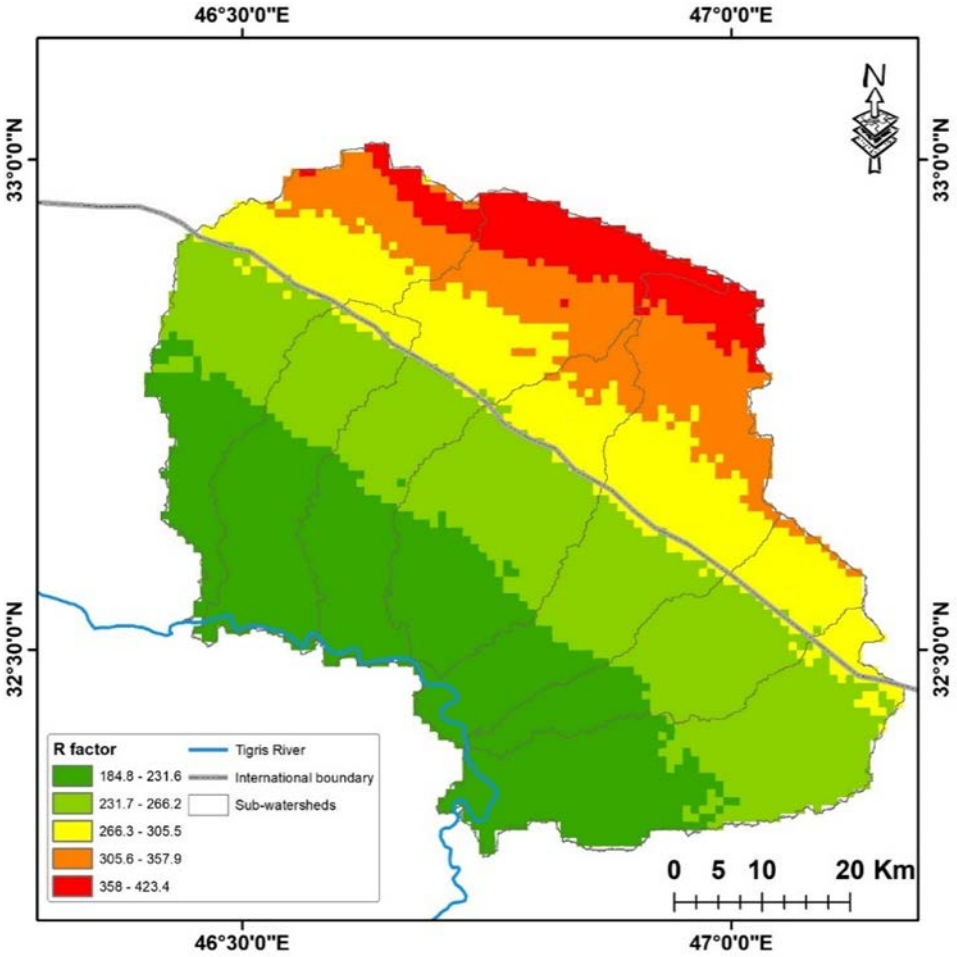

Figure 3. Map of rainfall erosivity in (MJ mm ha^{-1} h^{-1} yr^{-1}).

Table 4. *K* values for the study area.

Soil texture	SNUM	Soil composition			OM	K
		Sand	Silt	Clay		
Loam	3122	40	39	21	2.01	0.26
Clay	3136	37	46	17	5.40	0.21
Clay	3254	18	61	21	60.66	0.21
Loamy Sand	3529	86	10	4	3.38	0.04
Clay Loam	3554	40	39	21	2.01	0.28
Clay	3627	26	63	11	1.97	0.33
Clay	3634	37	46	17	5.40	0.21

Preprints (www.preprints.org) | NOT PEER-REVIEWED | Posted: 16 November 2022 doi:10.20944/preprints202211.0298.v1

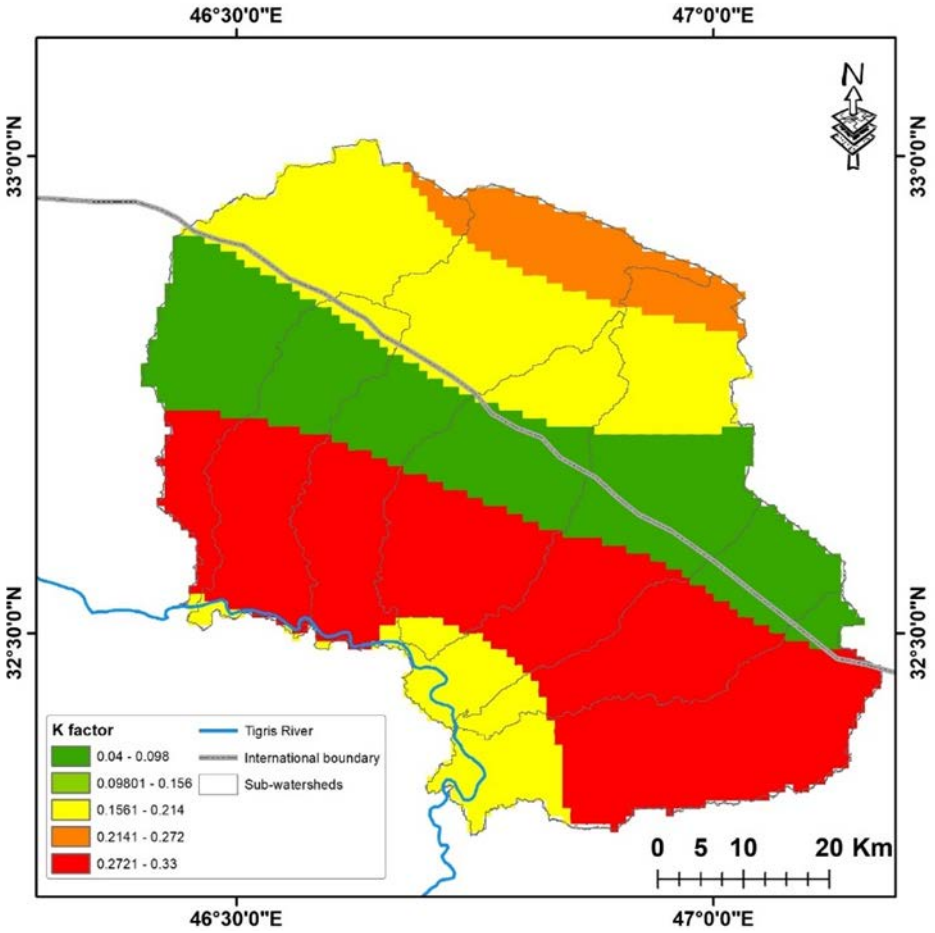

Figure 4. Soil erodibility (*K* factor) (tons ha^{-1} h^{-1} MJ mm^{-1}).

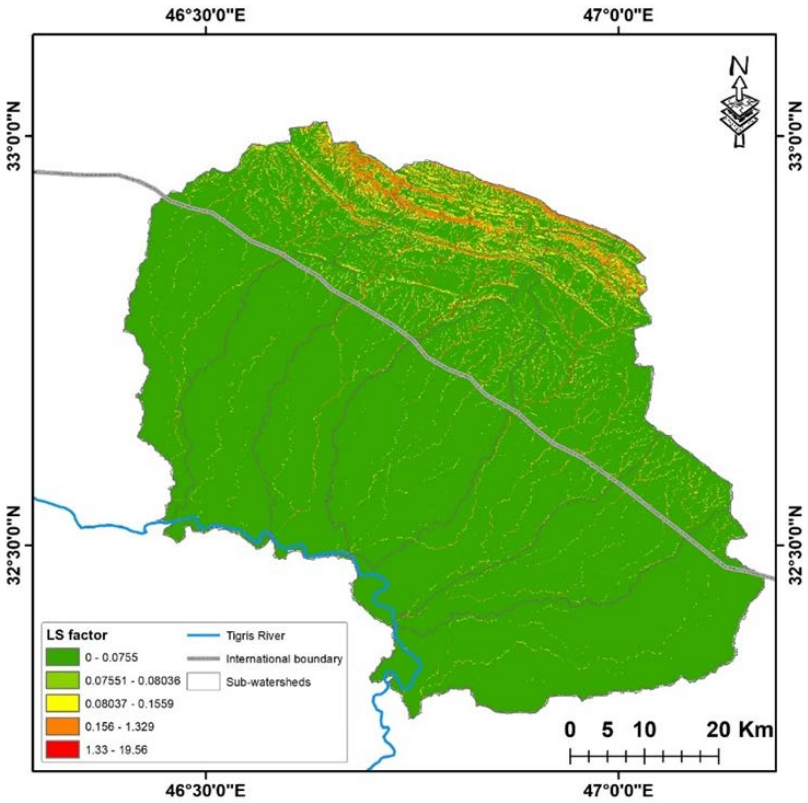

Preprints (www.preprints.org) | NOT PEER-REVIEWED | Posted: 16 November 2022 doi:10.20944/preprints202211.0298.v1

Figure 5. *LS* factor (dimensionless) map.

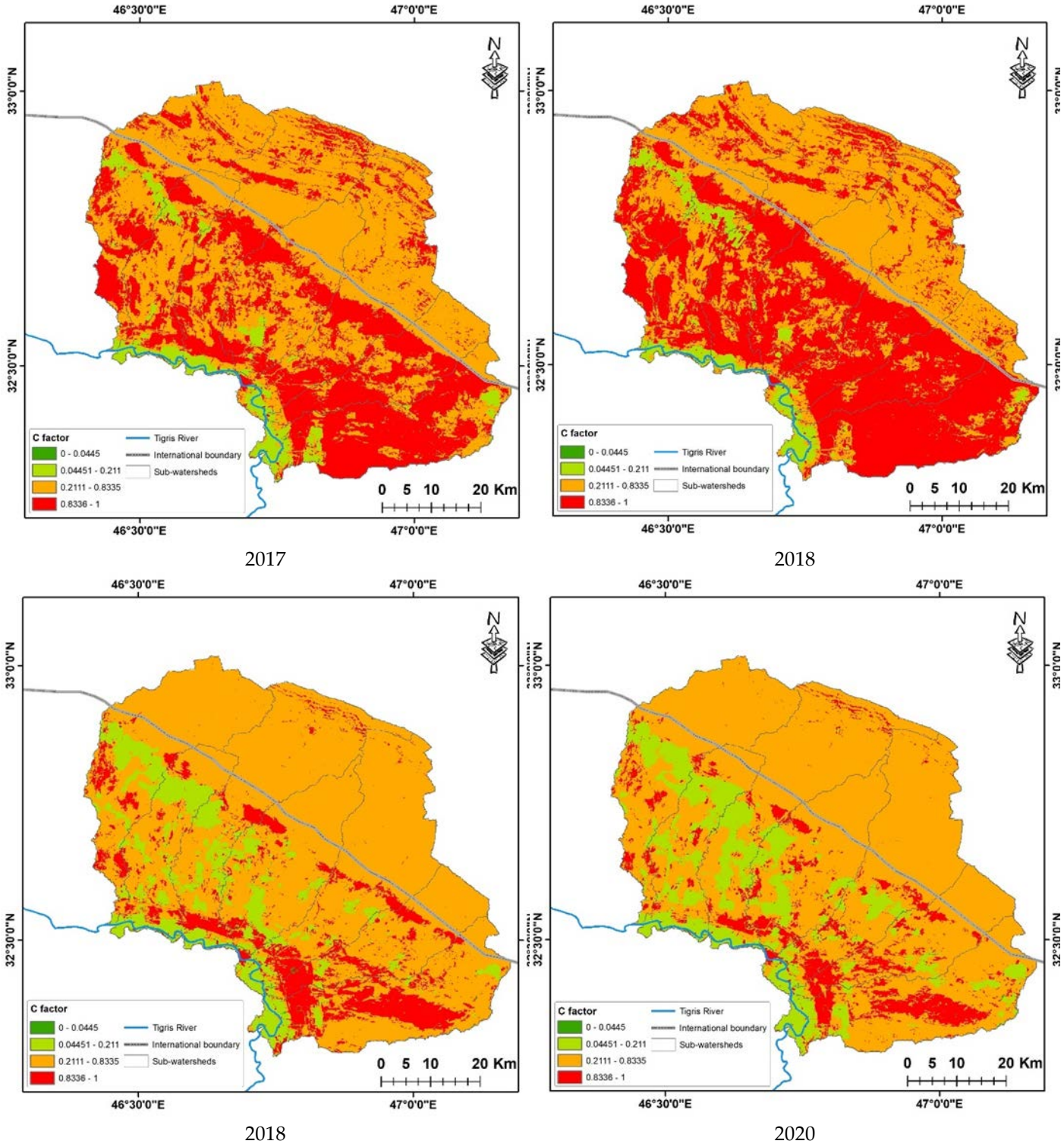

Figure 6. Spatial distribution of *C* factor for the node years.

Preprints (www.preprints.org) | NOT PEER-REVIEWED | Posted: 16 November 2022 doi:10.20944/preprints202211.0298.v1

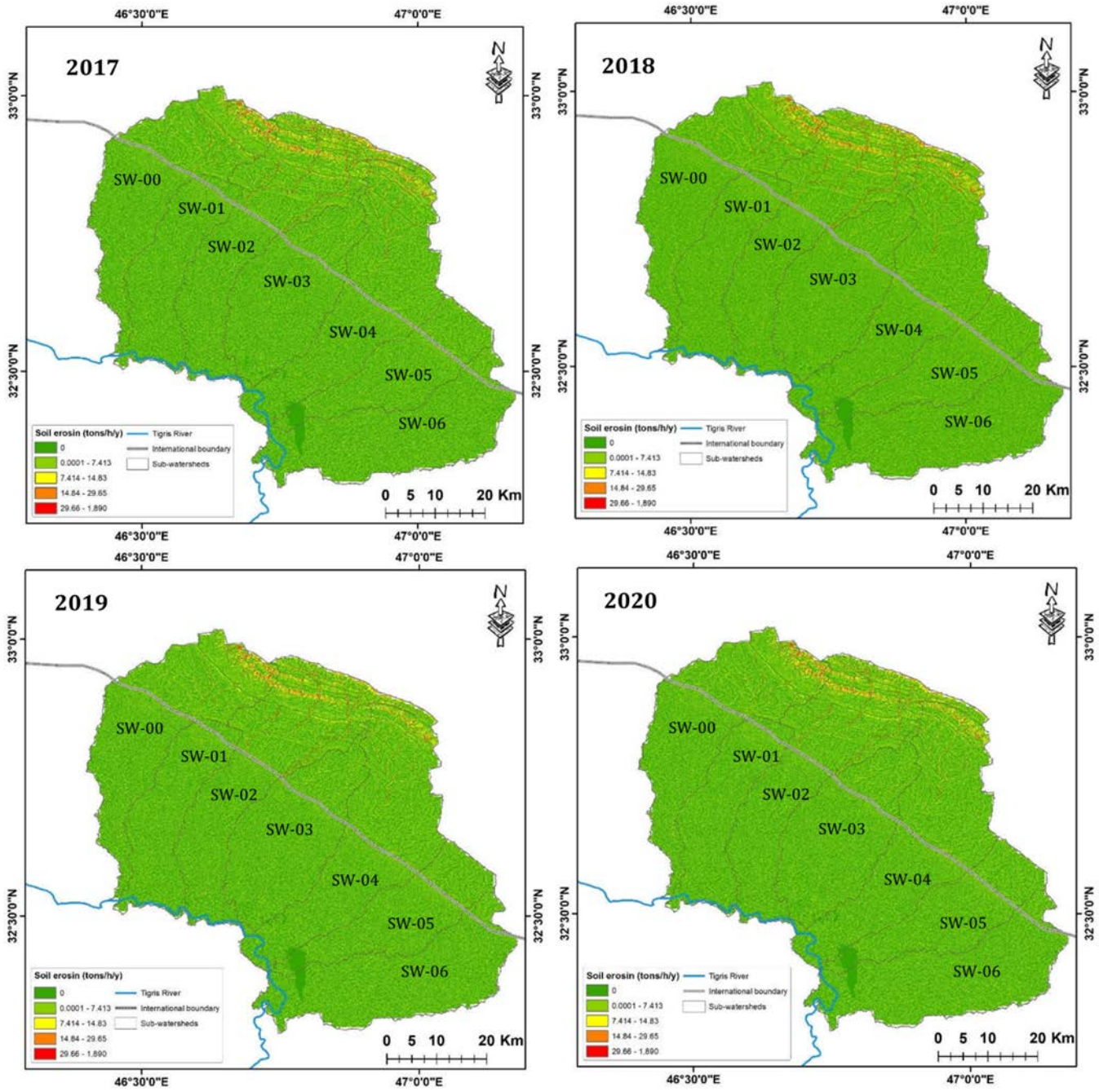

Figure 6. Soil erosion maps for the four node years.

4. Conclusions

This study demonstrated the use of RULSE soil loss model in conjunction with RS and GIS technologies to estimate the potential of soil erosion and priorities of transboundary of sub-watersheds at Northeastern Maysan Governorate, southern Iraq in terms of erosion conservation practices. The effects of changing LULS on erosion loss were also investigated. Results of the soil loss model indicate that the annual average loss range 0 - 1890 (tons h^{-1} y^{-1}). The amount of soil spatially varies significantly, with the northern and northeastern parts of sub-watersheds inside the Iranian land (the mountain and steep slope areas) is more prone to erosion than the plain southern and southwestern areas at the Iraqi land. Additionally, results confirmed that the northern portions of the SW-00,

SW-02, and SW-04 watersheds require high priority conservation plans; however, these portions are primarily located in mountainous areas, making it difficult to implement conservation plans there. Due to low soil loss, other sub-watersheds, like SW-01, SW-03, SW-05, and SW-06, are given a low priority. Findings of this study also show that *R* and *LS* were the more soil loss model factors affecting soil erosion than other components.

It is suggested that future work include a more appropriate *P* factor and use more advanced and high-resolution satellite imagery to reveal vegetation cover across the study area, which is a critical component to preventing soil loss and watershed priority against erosion. Additionally, the final soil loss model should include gully erosion type to correct spatially zone soil loss and suggest right conversation plans.

Author Contributions: Collected the data and carried out the investigation, A.A.; project administration, conceived and designed the study, A.M.; software analyzed the data and funding acquisition, H.A.; writing—original draft preparation, A.M.; writing—review, and editing, F.K.; visualization, S.H. All authors have read and agreed to the published version of the manuscript.

Funding: This research was supported by the Researchers Supporting Project number (RSP2022R425), King Saud University, Riyadh, Saudi Arabia.

Institutional Review Board Statement: Not applicable.

Informed Consent Statement: Not applicable.

Data Availability Statement: No new data were created or analyzed in this study. Data sharing is not applicable to this article.

Conflicts of Interest: The authors declare no conflict of interest

References

1. Vahabi, J., & Nikkami, D. Assessing dominant factors affecting soil erosion using a portable rainfall simulator. *International Journal of Sediment Research* **2008**, 23(4), 376-386. doi:10.1016/s1001-6279(09)60008-1
2. Borrelli, P., Ballabio, C., Panagos, P., & Montanarella, L. Wind erosion susceptibility of European soils. *Geoderma* **2014**, 232-234, 471-478. doi:10.1016/j.geoderma.2014.06.008
3. Lin, D., Shi, P., Meadows, M., Yang, H., Wang, J., Zhang, G., & Hu, Z. Measuring compound soil erosion by wind and water in the eastern agro–pastoral Ecotone of northern China. *Sustainability* **2022**, *14*(10), 6272. doi:10.3390/su14106272
4. Fagbohun, B. J., Anifowose, A. Y., Odeyemi, C., Aladejana, O. O., & Aladeboyeje, A. I. GIS-based estimation of soil erosion rates and identification of critical areas in Anambra sub-basin, Nigeria. *Modeling Earth Systems and Environment* **2016**, 2(3). doi:10.1007/s40808-016-0218-3
5. Gelder, B., Sklenar, T., James, D., Herzmann, D., Cruse, R., Gesch, K., & Laflen, J. The Daily erosion project - daily estimates of water runoff, soil detachment, and erosion. *Earth Surface Processes and Landforms* **2017,** 43(5), 1105-1117. doi:10.1002/esp.4286
6. Ahmad, N. S., Mustafa, F. B., Muhammad Yusoff, S. , & Didams, G. A systematic review of soil erosion control practices on the agricultural land in Asia. *International Soil and Water Conservation Research* **2020**, 8(2), 103-115. doi:10.1016/j.iswcr.2020.04.001
7. Prasannakumar, V., Vijith, H., Abinod, S., & Geetha, N. Estimation of soil erosion risk within a small mountainous sub-watershed in Kerala, India, using revised universal soil loss equation (RUSLE) and geo-information technology. *Geoscience Frontiers* **2012**, 3(2), 209-215. doi:10.1016/j.gsf.2011.11.003
8. Chowdary, V. M., Chakraborthy, D., Jeyaram, A., Murthy, Y. V., Sharma, J. R., & Dadhwal, V. K. Multi-criteria decision making approach for watershed prioritization using analytic hierarchy process technique and GIS. *Water Resources Management* **2013**, 27(10), 3555-3571. doi:10.1007/s11269-013-0364-6
9. Aher, P., Adinarayana, J., & Gorantiwar, S. Quantification of morphometric characterization and prioritization for management planning in semi-arid tropics of India: A remote sensing and GIS approach. *Journal of Hydrology* **2014**, 511, 850-860. doi:10.1016/j.jhydrol.2014.02.028
10. Khan, M., Gupta, V., & Moharana, P. Watershed prioritization using remote sensing and geographical information system: A case study from Guhiya, India. *Journal of Arid Environments* **2001**, 49(3), 465-475. doi:10.1006/jare.2001.0797
11. Neitsch, S.L., Arnold, J.G., Kiniry, J.R., Williams, J.R. Soil and Water Assessment Tool Theoretical Documentation Version. Texas Water Resources Institute, 2009.
12. Schmidt, J., von Werner, M., Michael, A. EROSION 2D/3D — a computer model to simulate water erosion. Sächsische Landesanstalt für Landwirtschaft, Dresden, 1996. (in German).

13. Wischmeier, W.H., & Smith, D.D. Predicting rainfall-erosion losses: a guide to conservation planning. Agriculture Handbook #507. USDA, Washington, DC, 1978.
14. Renard, K. G., & Ferreira, V. A. RUSLE model description and database sensitivity. *Journal of Environmental Quality* **1993**, 22(3), 458-466. doi:10.2134/jeq1993.00472425002200030009x
15. Wang, G., Gertner, G., Fang, S., & Anderson, A. B. Mapping multiple variables for predicting soil loss by Geostatistical methods with TM images and a slope map. *Photogrammetric Engineering & Remote Sensing* **2003** , 69(8), 889-898. doi:10.14358/pers.69.8.889
16. Hoyos, N. Spatial modeling of soil erosion potential in a tropical watershed of the colombian Andes. *CATENA* **2005**, 63(1), 85-108. doi:10.1016/j.catena.2005.05.012
17. Terranova, O., Antronico, L., Coscarelli, R., & Iaquinta, P. Soil erosion risk scenarios in the Mediterranean environment using RUSLE and GIS: An application model for Calabria (southern Italy). *Geomorphology* **2009** , 112(3-4), 228-245. doi:10.1016/j.geomorph.2009.06.009
18. Mhangara, P., Kakembo, V., & Lim, K. J. Soil erosion risk assessment of the Keiskamma catchment, South Africa using GIS and remote sensing. *Environmental Earth Sciences* **2011** , 65(7), 2087-2102. doi:10.1007/s12665-011-1190-x
19. Atoma, H., Suryabhagavan, K. V., & Balakrishnan, M. Soil erosion assessment using RUSLE model and GIS in Huluka watershed, central Ethiopia. *Sustainable Water Resources Management* **2020**, 6(1). doi:10.1007/s40899-020-00365-z
20. Rahman, M. R., Shi, Z., & Chongfa, C. Soil erosion hazard evaluation—An integrated use of remote sensing, GIS and statistical approaches with biophysical parameters towards management strategies. *Ecological Modelling* **2009**, 220(13-14), 1724-1734. doi:10.1016/j.ecolmodel.2009.04.004
21. Haiyan, F., & Liying, S. Modelling soil erosion and its response to the soil conservation measures in the Black soil catchment, northeastern China. *Soil and Tillage Research* **2017**, 165, 23-33. doi:10.1016/j.still.2016.07.015
22. Lin, J., Lin, Y., Zhao, H., & He, H. Soil erosion processes and geographical differentiation in Shaanxi during 1980–2015. *Sustainability* **2022**, 14(17), 10512. doi:10.3390/su141710512
23. Bai, L., Wang, N., Jiao, J., Chen, Y., Tang, B., Wang, H., … Wang, Z. Soil erosion and sediment interception by check dams in a watershed for an extreme rainstorm on the Loess Plateau, China. *International Journal of Sediment Research* **2020**, 35(4), 408-416. doi:10.1016/j.ijsrc.2020.03.005
24. Eniyew, S., Teshome, M., Sisay, E., & Bezabih, T. Integrating RUSLE model with remote sensing and GIS for evaluation soil erosion in Telkwonz watershed, northwestern Ethiopia. *Remote Sensing Applications: Society and Environment* **2021**, 24, 100623. doi:10.1016/j.rsase.2021.100623
25. Wang, H., & Zhao, H. Dynamic changes of soil erosion in the Taohe river basin using the RUSLE model and Google Earth engine. *Water* **2020**, 12(5), 1293. doi:10.3390/w12051293
26. Belayneh, M., Yirgu, T., & Tsegaye, D. Potential soil erosion estimation and area prioritization for better conservation planning in Gumara watershed using RUSLE and GIS techniques'. *Environmental Systems Research* **2019**, 8(1). doi:10.1186/s40068-019-0149-x
27. Tadesse, T. B., & Tefera, S. A. Comparing potential risk of soil erosion using RUSLE and MCDA techniques in central Ethiopia. *Modeling Earth Systems and Environment* **2020**, 7(3), 1713-1725. doi:10.1007/s40808-020-00881-z
28. Zhou, W., & WU, B. Assessment of soil erosion and sediment delivery ratio using remote sensing and GIS: A case study of upstream Chaobaihe river catchment, north China. *International Journal of Sediment Research* **2008**, 23(2), 167-173. doi:10.1016/s1001-6279(08)60016-5
29. Alexakis, D. D., Hadjimitsis, D. G., & Agapiou, A. Integrated use of remote sensing, GIS and precipitation data for the assessment of soil erosion rate in the catchment area of "Yialias" in Cyprus. *Atmospheric Research* **2013** , 131, 108-124. doi:10.1016/j.atmosres.2013.02.013
30. Abdo, H., & Salloum, J. Spatial assessment of soil erosion in Alqerdaha basin (Syria). *Modeling Earth Systems and Environment* **2017**, 3(1). doi:10.1007/s40808-017-0294-z
31. Rahi, K. A., Al-Madhhachi, A. T., & Al-Hussaini, S. N. Assessment of surface water resources of eastern Iraq. *Hydrology* **2019**, 6(3), 57. doi:10.3390/hydrology6030057
32. Sanchez, P. A., Ahamed, S., Carré, F., Hartemink, A. E., Hempel, J., Vanlauwe, B., Walsh, M. G., ... Zhang, G. L. Digital Soil Map of the World. Science, 325(5941), 680-681. https://doi.org/10.1126/science.1175084, 2009.
33. Fouad, S. F. A. Tectonic and structural evolution of the Mesopotamia Foredeep, Iraq. *Iraqi Bull. Geol* **2010**, (6)2, 41–53.
34. Falcon, N. (1974). Zagros mountains, Mesozoic-Cenozoic orogenic belts. Geol. Soc. , 4, 199-211.
35. Le Garzic, E., Vergés, J., Sapin, F., Saura, E., Meresse, F., & Ringenbach, J. Evolution of the NW Zagros fold-and-Thrust belt in Kurdistan region of Iraq from balanced and restored crustal-scale sections and forward modeling. *Journal of Structural Geology* **2019**, 124, 51-69. doi:10.1016/j.jsg.2019.04.006
36. Renard, K. G., & Foster, G. R. Soil conservation: principles of erosion by water. *Dryland agriculture* **1983**, 155-176.
37. Renard, K. G., & Freimund, J. R. Using monthly precipitation data to estimate the R-factor in the revised USLE. *Journal of Hydrology* **1994**, 157(1-4), 287-306. doi:10.1016/0022-1694(94)90110-4
38. Fu, G., Chen, S., & McCool, D. K.. Modeling the impacts of no-till practice on soil erosion and sediment yield with RUSLE, SEDD, and ArcView GIS. *Soil and Tillage Research* **2006**, 85(1-2), 38-49. doi:10.1016/j.still.2004.11.009

39. Panagos, P., Borrelli, P., Meusburger, K., Yu, B., Klik, A., Jae Lim, K., … Ballabio, C. Global rainfall erosivity assessment based on high-temporal resolution rainfall records. Scientific Reports 2017, 7(1). doi:10.1038/s41598-017-04282-8
40. Wischmeier, W. H., & Smith, D. D. A Universal Soil-Loss Estimating Equation to Guide Conservation Form Planning. 7 th Conger. Intern. Soil Sci. Soc. Trans, vol. 1, no. 2, 1961.
41. Roose, E. Land husbandry: components and strategy, vol. 70. FAO Rome,1996.
42. Moore, I. D., & Wilson, J. P. Length-slope factors for the revised universal soil loss equation: simplified method of estimation. *Journal of Soil and Water Conservation* **1992**, 47(5), 423 - 428.
43. Moore, I. D. & Burch, G. J. Modelling erosion and deposition: Topographic effects. *Transactions of the ASAE* **1986**, 29(6), 1624-1630. doi:10.13031/2013.30363
44. Das, G. Hydrology and soil conservation engineering: Including watershed management. PHI Learning Pvt. 2008.
45. Shalini Tirkey, A., Pandey, A., & Nathawat, M. Use of satellite data, GIS and RUSLE for estimation of average annual soil loss in Daltonganj watershed of Jharkhand (India). *Journal of Remote Sensing Technology* **2013**, 20-30. doi:10.18005/jrst0101004
46. Renard, K. G. Predicting soil erosion by water: A guide to conservation planning with the revised universal soil loss equation (RUSLE). United States Government Printing, 1997.
47. Namdar, F., Mahmoudi, S., Esmali Ouri, A., & Pazira, E. Investigating the effect of land use changes on soil erosion using RS-GIS and AHP-fuzzy based techniques (Case study: Qaresu watershed, Ardabil, Iran). *Nexo Revista Científica* **2020**, 33(02), 525-538. doi:10.5377/nexo.v33i02.10789
48. Addis, H. K., & Klik, A. Predicting the spatial distribution of soil erodibility factor using USLE nomograph in an agricultural watershed, Ethiopia. *International Soil and Water Conservation Research* **2015**, 3(4), 282-290. doi:10.1016/j.iswcr.2015.11.002
49. Benavidez, R., Jackson, B., Maxwell, D., & Norton, K. A review of the (Revised) universal soil loss equation ((R)USLE): With a view to increasing its global applicability and improving soil loss estimates. *Hydrology and Earth System Sciences* **2018**, 22(11), 6059-6086. doi:10.5194/hess-22-6059-2018
50. Doulabian, S., Shadmehri Toosi, A., Humberto Calbimonte, G., Ghasemi Tousi, E., & Alaghmand, S. Projected climate change impacts on soil erosion over Iran. *Journal of Hydrology* **2021**, 598, 126432. doi:10.1016/j.jhydrol.2021.126432
51. Zhang, H., Yang, Q., Li, R., Liu, Q., Moore, D., He, P., … Geissen, V. Extension of a GIS procedure for calculating the RUSLE equation LS factor. *Computers & Geosciences* **2013**, 52, 177-188. doi:10.1016/j.cageo.2012.09.027
52. Schmidt, S., Tresch, S., & Meusburger, K. Modification of the RUSLE slope length and steepness factor (LS-factor) based on rainfall experiments at steep Alpine grasslands. *MethodsX* **2019**, 6, 219-229. doi:10.1016/j.mex.2019.01.004
53. Zhou, P., Luukkanen, O., Tokola, T., & Nieminen, J. Effect of vegetation cover on soil erosion in a mountainous watershed. *CATENA* **2008**, 75(3), 319-325. doi:10.1016/j.catena.2008.07.010
54. Fan, J., Motamedi, A., & Galoie, M. Impact of C factor of USLE technique on the accuracy of soil erosion modeling in elevated mountainous area (case study: The Tibetan Plateau). Environment, *Development and Sustainability* **2021**, 23(8), 12615-12630. doi:10.1007/s10668-020-01133-x
55. Jenks, G. F. The data model concept in statistical mapping. Int. Yearb. Cartogr, 7, 186 –190, 1967.
56. El-Hassanin, A., Labib, T., & Gaber, E. Effect of vegetation cover and land slope on runoff and soil losses from the watersheds of Burundi. Agriculture, *Ecosystems & Environment* **1993**, 43(3-4), 301-308. doi:10.1016/0167-8809(93)90093-5
57. Ziadat, F. M., & Taimeh, A. Y. Effect of rainfall intensity, slope, land use and antecedent soil moisture on soil erosion in an arid environment. *Land Degradation & Development* **2013**, 24(6), 582-590. doi:10.1002/ldr.2239